sitions to or from flat energy bands and nondirect transitions. However, the resolution of photoemission data is approximately 0.1 eV. Hence, a band would have to vary over less than 0.1 eV before this ambiguity would arise. The five $d$ bands in copper, for instance, extend over 3.5 eV, so this problem should not be important in this material. In materials where bands are narrower than 0.1 eV, it is evident that the concepts of direct transitions and Bloch waves lose their importance, since the wave functions are probably represented more accurately in terms of atomic orbitals.

In the following article, photoemission measurements of copper and silver which illustrate most of the effects described here are presented and interpreted.

PHYSICAL REVIEW VOLUME 136, NUMBER 4A 16 NOVEMBER 1964

# Photoemission Studies of Copper and Silver: Experiment*†

C. N. BERGLUND‡ AND W. E. SPICER
*Stanford Electronics Laboratories, Stanford University, Stanford, California*
(Received 22 June 1964)

Experimental photoemission data from copper and silver are presented and interpreted in detail in terms of the calculated band structures over a photon energy range from 1.5 to 11.5 eV. It is shown that nondirect optical transitions are stronger than direct ones in both metals. In fact, the only direct optical transitions observed are rather weak ones between $p$- and $s$-like states near $L_2'$ and $L_1$ in the calculated band structures. No evidence of direct transitions from the $d$ bands is found. From the data, the density of states for copper and silver is determined from approximately 7 eV below the Fermi level to approximately 10 eV above it. Several symmetry points in the calculated band structures, and the $d$ bands, are located absolutely in energy. It is found that electron-electron scattering is the dominant inelastic scattering mechanism for energetic electrons in the metals over the range of energy studied. No evidence of electron scattering by plasmon creation is found. In the silver data, the Auger process is identified, and its effect on photoemission is discussed in detail. To check on the results and conclusions drawn from the photoemission studies, and to illustrate the utility of the method, the spectral distribution of the quantum yield and the energy distribution of photoemitted electrons at several photon energies for copper are calculated and compared to the observations. The contribution of the Auger process to photoemission is calculated and compared to the observations for silver. In addition, the imaginary part of the dielectric constant $\epsilon_2$ for both copper and silver is calculated, assuming that only nondirect optical transitions are important, and compared to measured values. In all cases, very good agreement is obtained.

## I. INTRODUCTION

IN the previous paper,[1] the effects of different optical transitions and electron scattering processes on photoemission from metals have been described. In this paper, experimental data from the metals copper and silver are presented which illustrate most of these effects. The data are interpreted in detail in terms of the calculated band structures of the metals. In this paper, as in the preceding one, optically excited electronic transitions in which direct conservation of $k$ vector is not required are referred to as nondirect transitions.

A description of the instrumentation used is given elsewhere.[2] The phototubes used were of the same design as those used by Apker *et al.*,[3] and Spicer.[4] The metals were evaporated onto the photocathode and collector in vacuum to a thickness of approximately 2000 to 5000 Å. Following evaporation of the metal, approximately a monolayer of cesium was deposited on the surface of the metals to reduce the work function to values of 1.55 and 1.65 eV for copper and silver, respectively. The optimum layer of cesium on the metal surface was determined by maximizing the photoemission from the metal when it was irradiated with light from a tungsten lamp.

In order to verify that the cesium layer had no effect on the photoemission results other than the reduction in work function, a copper phototube was constructed without cesium treatment. The experimental results from this tube were consistent with the results reported here for tubes with cesium on the surface.

## II. PHOTOEMISSION STUDY OF COPPER

### A. The Calculated Band Structure of Copper

Calculations of the energy band structure of copper have recently been made by Segall and Burdick.[5,6] It is

* Work supported by the Advanced Research Projects Agency through the Center for Materials Research at Stanford University, Stanford, California.

† Based on a thesis submitted by C.N.B. to Stanford University in partial fulfillment of the requirements of the Ph.D. degree.

‡ Present address: Bell Telephone Laboratories, Murray Hill, New Jersey.

[1] C. N. Berglund and W. E. Spicer, Phys. Rev. **136**, A1030 (1964), preceding paper.

[2] W. E. Spicer and C. N. Berglund (to be published).

[3] L. Apker, E. Taft, and J. Dickey, J. Opt. Soc. Am. **43**, 78 (1953).

[4] W. E. Spicer, Phys. Chem. Solids **22**, 365 (1961).

[5] B. Segall, Phys. Rev. **125**, 109 (1962).

[6] G. A. Burdick, Phys. Rev. **129**, 138 (1963).

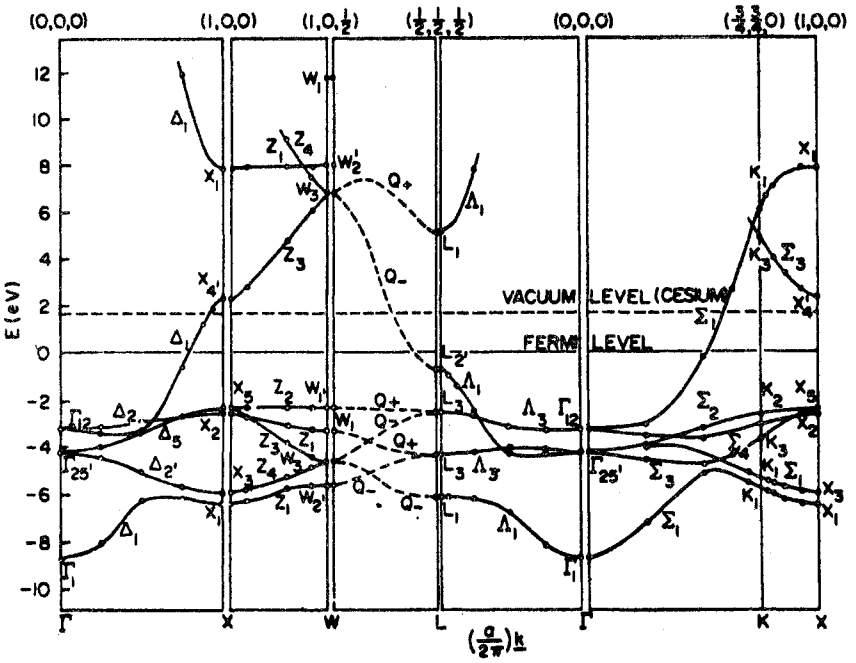


FIG. 1. Calculated band structure of copper, after Segall (Ref. 5).

of importance to describe the crystal potentials which were used in these calculations, since the extremely close agreement between many of the features of the calculated band structure and the experimental results reported here indicates that the potential was very accurately approximated.

In Segall's work, the band structure was calculated twice by the Green's function method[7] using two different potentials. One of the potentials used was that constructed by Chodorow.[8] This potential yields the $3d$-electron Hartree-Fock functions for the free $Cu^+$ ion. To this Segall added the contribution of a "metallic" $s$-electron function (the $s$ function for an electron of average energy). The use of this potential implies the Wigner-Seitz approximation that all conduction electrons, except those for the unit cell under consideration, are excluded from the cell by correlation and exchange interactions. The potential might be expected to be most accurate for the $d$ electrons. Also, it includes the approximation that the same potential applies to all angular momentum components of the wave function.

The core and $d$-electron Hartree-Fock functions for neutral copper were renormalized in the Wigner-Seitz sphere and used for the second potential. The Coulomb and exchange contributions to the potential for the various values of $l$ were computed for a configuration which included, in addition to the core and $d$ electrons, a renormalized $s$ function.

Segall found that the band structures calculated for the two different potentials were very similar. The positions of the bands were somewhat different, but the general features were the same.

Burdick calculated the band structure by the augmented-plane-wave (APW) method[9] using the Chodorow potential described above. His results agreed with those of Segall for the same potential to within 0.15 eV.

The band structure along the various symmetry axes in the reduced zone calculated by Segall using the $l$-dependent potential is shown in Fig. 1. This band structure will be used in discussing the photoemission data. (Detailed comparisons of the data to the calculations of both Segall and Burdick will be given in the text.) In Fig. 1 the points of symmetry are labeled ac-

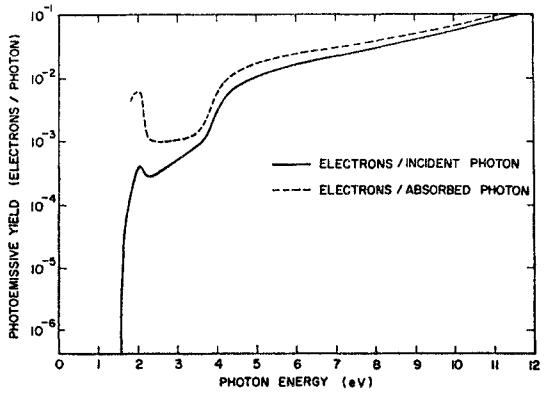


FIG. 2. Quantum yield of copper.

[7] W. Kohn and N. Rostoker, Phys. Rev. **94**, 1111 (1954).
[8] M. Chodorow, Phys. Rev. **55**, 675 (1939); Ph.D. thesis, MIT, 1939 (unpublished).
[9] J. C. Slater, Phys. Rev. **51**, 846 (1937); **92**, 603 (1953).

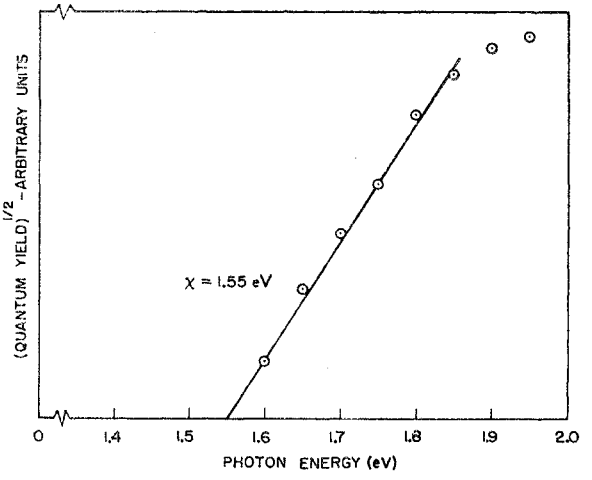


FIG. 3. Evaluation of work function of copper with cesium on the surface.

cording to the notation of Bouckaert, Smoluchowski, and Wigner.[10] The relatively flat bands located approximately 2 to 6 eV below the Fermi level originate principally from the atomic $d$ bands, and, for the sake of simplicity, will be referred to in this paper as the $d$ bands. The other bands will be referred to as the $p$- and $s$-like bands. Because of the flatness of the $d$ bands, they are characterized by a relatively high density of states. The difference in energy between the vacuum level marked on the figure and the Fermi level is the work function of copper with approximately a monolayer of cesium on the surface. This energy is determined by studying the quantum yield of a suitably treated copper photoemitter as a function of photon energy.

### B. The Quantum Yield

Figure 2 shows the quantum yield of copper with approximately a monolayer of cesium on the surface. The solid curve is the measured yield per incident photon, corrected for the transmission of the LiF window of the phototube. The dashed curve is the yield per absorbed photon determined from the measured yield and the reflectivity of copper.[11]

In a theoretical treatment of photoemission from metals, Fowler[12] has derived the following equation for the quantum yeild near the threshold of photoemission:

$$\begin{aligned} Y &\propto (h\nu-\chi)^2 \quad h\nu \gtrsim \chi, \\ &= 0 \qquad\quad h\nu < \chi, \end{aligned} \tag{1}$$

where $\chi$ is the work function of the metal. By Eq. (1), a plot of the square root of the yield as a function of photon energy should give a straight line extrapolating to the work function at zero field. Such a plot for copper with the optimum Cs treatment is shown in Fig. 3. The work function determined from Fig. 3 is 1.55 eV.

The general features of the quantum yield curve shown in Fig. 2 are due to the $d$ bands. This can most easily be demonstrated by the following argument. If scattering effects are negligible, the quantum yield can be written approximately as[13]

$$Y \propto \alpha_a/(\alpha_a+\alpha_b), \tag{2}$$

where $\alpha_a$ is that part of the absorption coefficient due to transitions to states above the vacuum level, and $\alpha_b$ is that part due to transitions to states between the Fermi level and the vacuum level. The decrease in yield in Fig. 2 at about 2.1-eV photon energy is due principally to an increase in $\alpha_b$, since this photon energy is the threshold for transitions from the $d$ band to states just above the Fermi surface. At 3.7-eV photon energy, $d$-band electrons can be excited to states above the vacuum level resulting in an increase in $\alpha_a$ and in the yield. The slow increase in yield at photon energies greater than 6 eV is due to scattering, and will be explained in detail in Sec. G.

### C. Energy Distribution of Photoemitted Electrons—$h\nu < 3.7$ eV

At photon energies less than 3.7 eV, electrons excited from the $d$ bands do not gain enough energy to escape, and structure in the energy distribution of photoemitted electrons is due to transitions from the $p$- and $s$-like states just below the Fermi level to $p$- and $s$-like states just above the vacuum level. Details of the band structure in these energy regions can be determined by studying the energy distribution of photoemitted electrons.

Figure 4 shows the energy distributions which result for photon energies from 2.1 to 3.7 eV. Two peaks appear in the distribution, one fixed in energy indepen-

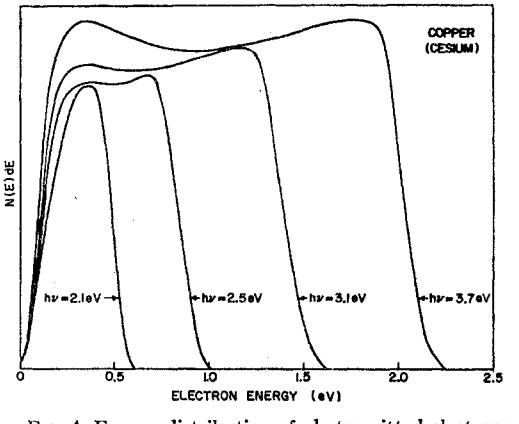


FIG. 4. Energy distribution of photoemitted electrons from copper—$h\nu < 3.7$ eV.

[10] L. P. Bouckaert, R. Smoluchowski, and E. Wigner, Phys. Rev. **50**, 58 (1936).
[11] H. Ehrenreich and H. R. Philipp, Phys. Rev. **128**, 1622 (1962).
[12] R. H. Fowler, Phys. Rev. **38**, 45 (1931).
[13] W. E. Spicer, J. Appl. Phys. **31**, 207 (1960).

dent of $h\nu$ at about 0.25 eV above the vacuum level, and the other with energy $E$ given by

$$E=h\nu-1.90\text{ eV}. \quad (3)$$

The two peaks coincide at a photon energy of approximately 2.1 eV.

The behavior shown in Fig. 4 is characteristic of nondirect transitions and can be explained in terms of two peaks in the density of states. The explanation of these particular transitions has been given in the preceding paper.[1] Assuming a work function of 1.55 eV, the peaks in the density of states are located 0.35 eV below and 1.8 eV above the Fermi level.

Comparing this experimentally determined density of states to the calculated band structure in Fig. 1, it is evident that the peak 0.35 eV below the Fermi level is associated with the high density of states near the symmetry point $L_2'$, and that the peak 1.8 eV above the Fermi level is associated with the high density of states near the symmetry point $X_4'$. Segall[5] and Burdick[6] indicate critical points at $X_4'$ (2.3 or 2.0 eV, respectively, above the Fermi surface) and at $L_2'$ (0.8 or 0.6 eV, respectively, below the Fermi surface). The energies at the symmetry points attributed to Segall are those calculated assuming the $l$-dependent potential.

It has been pointed out to the authors[14] that the location of symmetry point $L_2'$ 0.35 eV below the Fermi level, as determined from the data, is important and warrants further discussion and verification. (Previously, this symmetry point had been located approximately 0.7 eV below the Fermi level.)

In Sec. 4, direct transitions from $L_2'$ to $L_1$ will be identified which provide further evidence that $L_2'$ is 0.35 eV below the Fermi level. In addition to this, independent experimental work on thin Cu films evaporated onto semiconductors has shown anomalous results

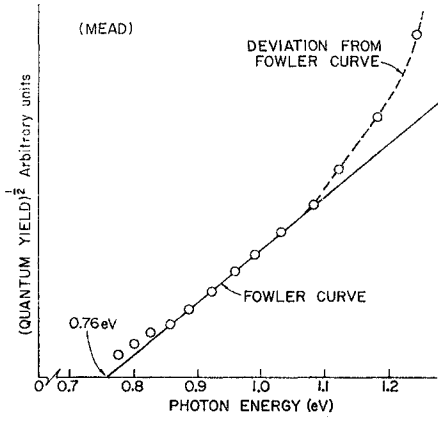


FIG. 5. Yield curve obtained by Mead and Spitzer (Ref. 15) from Cu on $n$-type GaAs. The solid line indicates a Fowler curve. For $h\nu>1.1$ eV, the experimental points lie above the Fowler curve. This would be expected if there were a high density of states located approximately 0.35 eV below the Fermi surface.

[14] J. C. Phillips (private communication).

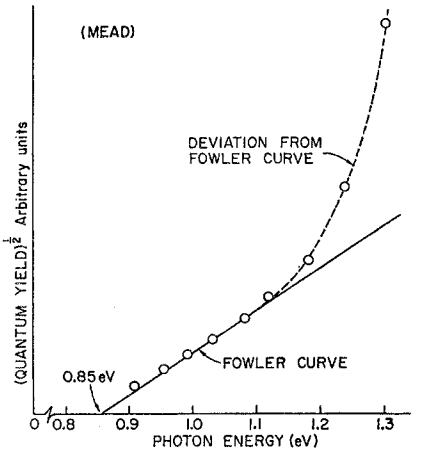


FIG. 6. Yield curve obtained by Mead and Spitzer from Ag on $n$-type GaAs (Ref. 15). The solid line indicates a Fowler curve. For $h\nu>1.15$ eV, the experimental points lie above the Fowler curve. This would be expected if there were a high density of states located approximately 0.3 eV below the Fermi surface.

which can be easily explained if a high density of states exists in Cu approximately 0.35 eV below the Fermi level.[15,16] In these experiments, light of photon energy below the band-gap energy of the semiconductor is directed onto the metal film and the number of electrons injected by the metal into the semiconductor per incident photon is measured as a function of photon energy. Near threshold, the spectral distribution of yield should follow Eq. (1). Figure 5 shows a plot obtained by Mead and Spitzer[15] of the square root of the quantum yield versus photon energy for Cu on $n$-type GaAs. At photon energies near threshold, the square root of the yield follows approximately a straight line as expected from Eq. (1), and gives a threshold energy of 0.76 eV. However, at photon energies above 1.1 eV (i.e., 0.34 eV above threshold), the square root of the yield increases sharply. This behavior is different from that expected from the Fowler theory.[12] In fact, the square root of the yield should become less than that given by the straight-line approximation at photon energies well above threshold, and this behavior is found in Al and Au.[17] It is evident that a square root of yield curve similar to that shown in Fig. 5 would be obtained if there was a peak in the copper density of states 0.34 eV below the Fermi level.

Figure 6 shows the square root of yield versus photon energy for silver on $n$-type GaAs. At photon energies approximately 0.3 eV above threshold, the curve increases sharply indicating a peak in the Ag density of states 0.3 eV below the Fermi level. It will be shown later that the photoemission data from silver also indicates a peak in the density of states 0.3 eV below the Fermi level which is attributed to symmetry point $L_2'$.

[15] C. A. Mead (private communication).

[16] P. Bardell (private communication).

[17] W. G. Spitzer and C. A. Mead, J. Appl. Phys. 34, 3061 (1963).

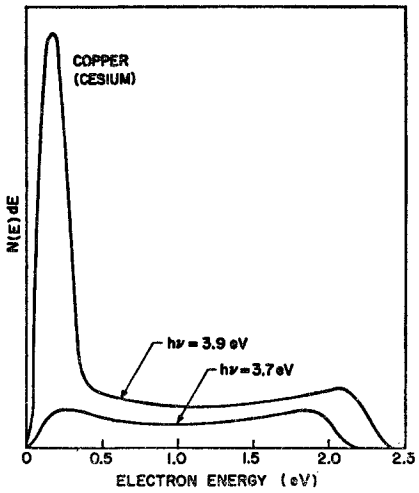


FIG. 7. Energy distribution of photoemitted electrons from copper—$h\nu=3.7$ eV, 3.9 eV.

In silver, $L_2'$ had previously been located more than 0.4 eV below the Fermi level. However, recent measurements by Joseph[18] locate it between 0.3 and 0.4 eV below the vacuum level.

An increase in the square root of yield near threshold due to $L_2'$ is not noted either in copper (Fig. 30) or silver (Fig. 31) in the present work. This is probably due to the fact that higher photon energies than those used by Bardell and Mead are used here. Interband transitions and changes in reflectivity could mask the effect at these higher photon energies.

### D. Transitions from the *d* Bands

At photon energies greater than 3.7 eV, electrons can be optically excited from the $d$ bands to states above the vacuum level. These electrons will appear in the energy distribution of the photoemitted electrons at these photon energies. Figure 7 shows the energy distribution for photon energies of 3.7 and 3.9 eV. At 3.7 eV there is very little evidence of $d$-band electrons being excited to states above the vacuum level. At 3.9 eV, however, a large number of slow electrons appear which can only be explained in terms of transitions from the $d$ bands. When the photon energy is further increased, as shown in Fig. 8, more of the $d$ bands become exposed.

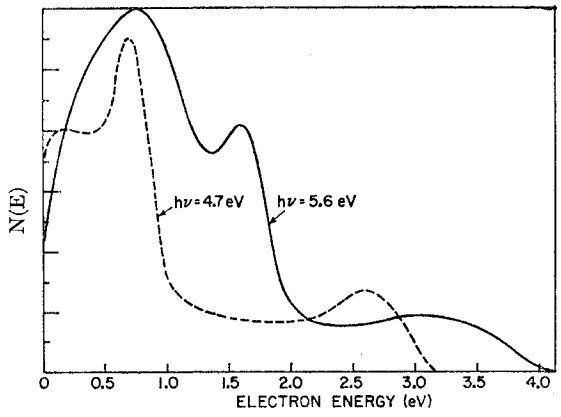


FIG. 8. Energy distribution of photoemitted electrons from copper—$h\nu=4.7$ eV, 5.6 eV.

[18] A. S. Joseph (private communication).

Two peaks in the $d$-band density of states are evident in Fig. 8. If the energy distribution of the photoemitted electrons from the $d$ bands is plotted versus $E-h\nu$ rather than versus $E$ as shown in Fig. 9 the energies of the two peaks in the distributions always coincide. According to the discussion in the preceding paper,[1] this behavior can only be explained if transitions from the $d$ bands are predominantly nondirect. This behavior cannot be explained in terms of the calculated band structure if direct transitions are assumed. Using a work function of 1.55 eV, the two peaks in the $d$ band are located 2.4 and 3.3 eV below the Fermi level and are approximately 0.2 eV wide and 1.0 eV wide, respectively. A detailed description of the $d$-band density of states and a comparison with the calculated density of states is given in Sec. F.

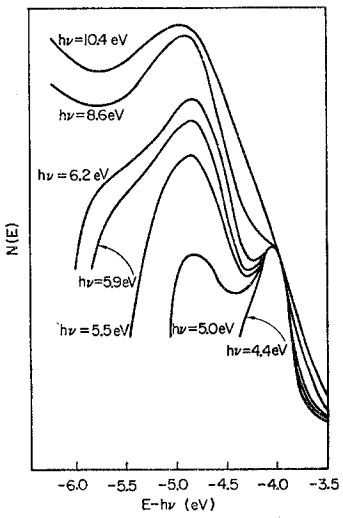


FIG. 9. Energy distribution of photoemitted electrons from copper plotted versus $E-h\nu$.

Figure 9 illustrates several scattering effects in addition to providing evidence that transitions from the $d$ band of copper are predominantly nondirect. The broadening of the peaks as they are excited to higher energies is apparent. This broadening suggests that the lifetime for scattering is strongly dependent on electron energy in agreement with previous experimental and theoretical work. The decrease in height of the narrow, higher-lying peak compared to that of the broad, lower lying peak with increased excitation energy is attributed to the energy dependence of the mean free path for scattering and to the fact that once-scattered electrons are contributing more to the lower-lying peak than to the higher lying peak. This is demonstrated by the

curves at photon energies of 8.6 and 10.4 eV where the contribution of once-scattered electrons at $E-h\nu<5.7$ eV can be seen. All of these effects will be described in detail later.

### E. Nondirect and Direct Transitions in Copper

It has been shown in Secs. B and C that transitions between $s$- and $p$-like states to states above the vacuum level for $h\nu<3.7$ eV, and transitions from the $d$ bands to $s$- and $p$-like states above the vacuum level can be adequately explained in terms of nondirect transitions. There is no evidence of direct transitions in these cases. However, for photon energies above 4.1 eV, direct transitions contribute to the observed results. Referring to Figs. 4, 7, and 8, the peak near the maximum electron energy attributed to transitions from $p$-like states near $L_2'$ grows in size at $h\nu=4.7$ eV, and becomes broader as

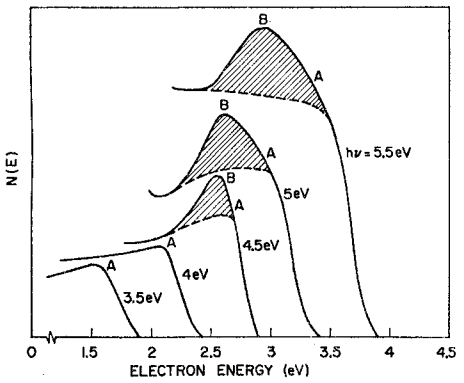


FIG. 10. Experimental evidence of direct and indirect transitions in copper. The contribution of direct transitions is indicated by the cross-hatched area.

shown for $h\nu=5.6$ eV. This behavior can be interpreted in terms of nondirect and direct transitions.

In the preceding paper,[1] the effects on photoemission measurements of direct and nondirect transitions between the $p$- and $s$-like states near $L_2'$ and $L_1$ in the calculated band structure have been described. In Fig. 10, portions of the energy distributions near the maximum electron energy where these transitions should be taking place are shown for several values of $h\nu$. By comparing these curves to the distributions which would result for direct and nondirect transitions given in the preceding paper, the fraction of electrons in the distribution due to direct transitions has been estimated, and is shown by the shaded areas in Fig. 10. (The estimate includes the distorting effect of the energy-dependent scattering described later.) It is evident that the probability of electrons being involved in nondirect transitions is somewhat stronger than the probability of their being involved in direct transitions in the copper samples studied here. This is the complete opposite of

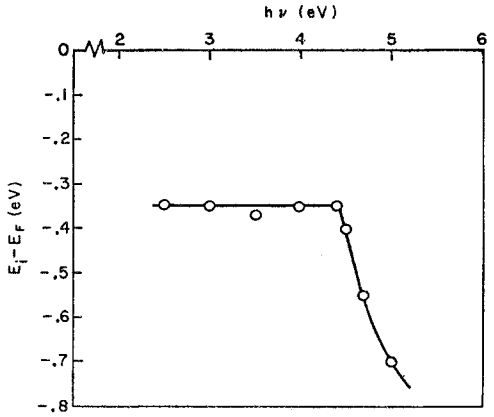


FIG. 11. Energy of initial states responsible for high-energy peak in photoemission data. The break at 4.4 eV is due to the onset of direct transitions.

the behavior in the semiconductors Si and Ge.[19] No other evidence of direct transitions in copper from other $p$- and $s$-like states, or from the $d$-like states was found over the range of electron energy studied.

The observation of direct transitions from states near $L_2'$ to states near $L_1$ can be used to determine accurately the energy of both symmetry points. In Fig. 11, the energies of the symmetry points are determined. The energy plotted vertically in the figure is the energy of the initial states responsible for the large peak in the energy distributions of Fig. 10. This energy is given by

$$E_i=E_F+E-h\nu+1.55\text{ eV}, \qquad (4)$$

where $E$ is the energy at the peak in Fig. 10. For $h\nu$ less than 4.4 eV, the energy $E_i-E_F$ is constant at $-0.35$

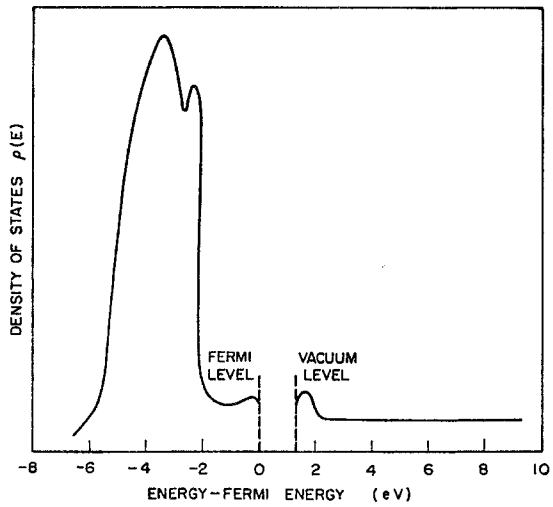


FIG. 12. First estimate of Cu density of states.

[19] D. Brust, J. C. Phillips, and F. Bassani, Phys. Rev. Letters 9, 94 (1962); D. Brust, M. L. Cohen, and J. C. Phillips, *ibid.* 9, 389 (1962).

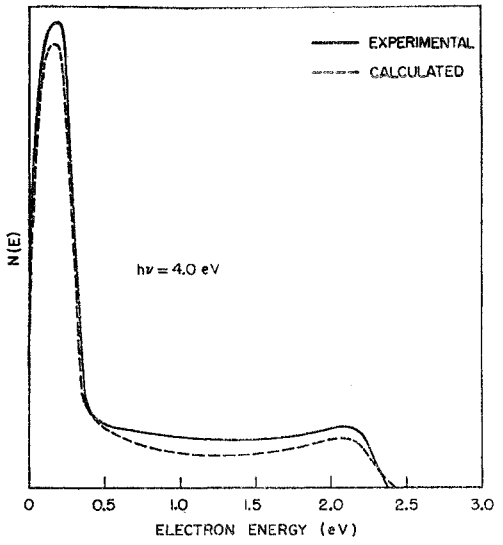


FIG. 13. Calculated and measured energy distribution of photoemitted electrons—$h\nu = 4.0$ eV.

eV, indicating that the peak in the distributions is due to a peak in the density of states 0.35 eV below the Fermi level. At $h\nu = 4.4$ eV, the energy $E_i - E_F$ breaks away from $-0.35$ eV and becomes rapidly more negative as $h\nu$ increases indicating an initial state which decreases in energy as $h\nu$ increases. As discussed in detail in the preceding paper,[1] this is the behavior to be expected for a direct transition. Hence, at $h\nu = 4.4$ eV, symmetry points $L_2'$ and $L_1$ must be joined in energy, and $L_1$ must be located 4.05 eV above the Fermi level. Segall and Burdick have located this point 5.1 and 4.2 eV above the Fermi surface, respectively.

### F. The Copper Density of States

It has been shown above that the energy distribution of photoemitted electrons from copper can be interpreted in terms of nondirect transitions except for the small contribution of direct transitions from states near $L_2'$ to states near $L_1$. Since the nondirect transition probability is proportional to the product of the initial and final density of states, it is possible to determine the relative density of states from the photoemission data.

The procedure followed in determining the density of states of copper in detail was one of trial and error. Many of the important features of the density of states can be determined without making a detailed analysis. For example, the energy location and shape of the $d$ band and of the peaks in the density of states 0.35 eV below and 1.8 eV above the Fermi level have been described in Secs. C and D. From this information, an estimate of the density of states can be made. This estimate is shown in Fig. 12. If the energy distributions of photoemitted electrons at several photon energies are calculated using this density of states and compared to the measured distributions, it is found that only small corrections to the density of states are required to bring the measured and predicted photoemission energy distributions into close agreement.

In order to predict the energy distribution of photoemitted electrons, information in addition to the density of states is required. That this is the case can be seen from the theoretical expression for the energy distribution which is reproduced here for convenience from the previous article.[1] This expression includes the effects of electron-electron scattering.

$$N_\nu(E)dE = \frac{KC(E)\alpha_\nu'(E)dE}{\alpha(\nu)+[1/l(E)]} \times\left[1+2\int_E^{E_F+h\nu}\frac{p_s(E',E)}{P_s(E')}\frac{\alpha_\nu'(E')}{\alpha_\nu'(E)}dE'\right]. \quad (5)$$

The threshold function $C(E)$ in copper is difficult to determine because the energy distribution curves are strongly affected by the peak in the density of states just above the vacuum level. However, $C(E)$ for silver is relatively easy to estimate, and will be used here (see Fig. 43). The absorption coefficient $\alpha(\nu)$ for copper is given in the literature.[11] The scattering parameters $p_s(E',E)$, $P_s(E')$, and $l(E)$ can be estimated using the density of states. (A detailed description of these calculations is given in Sec. G.) The function $\alpha_\nu'(E)$ is given in Eq. (29) of the previous paper, and for nondirect transitions is proportional to the product of the initial and final density of states if the matrix element joining the initial and final states is assumed constant.

Figures 13 and 14 show the measured and predicted energy distribution curves at two photon energies to illustrate the degree of accuracy obtained after corrections to the density of states have been made. The

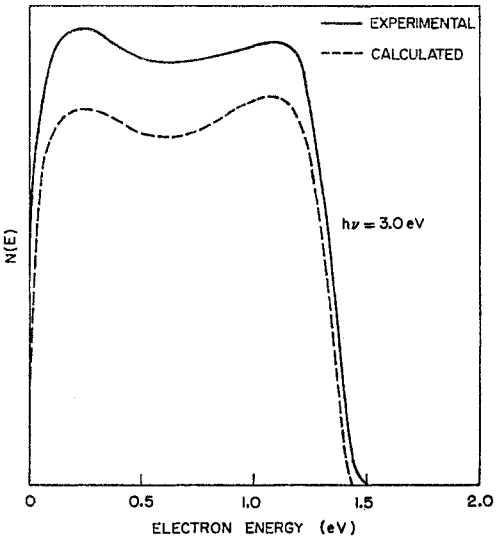


FIG. 14. Calculated and measured energy distribution of photoemitted electrons—$h\nu = 3.0$ eV.

curves were not normalized for best agreement because the curves would nearly coincide and be difficult to separate in the figures. These curves are indicative of the agreement obtained over the photon energy range from 2 to 11 eV. The excellent agreement indicates that the initial assumption of constant matrix element was reasonable, and that the density of states and the threshold function have been accurately estimated.

Only the density of states above the vacuum level and below the Fermi level can be determined by comparing calculated and measured energy distribution curves. However, the density of states between the Fermi level and the vacuum level can be estimated indirectly from the quantum yield curve. At electron energies up to several electron volts above the vacuum level, scattering is nearly negligible in copper and Eq. (60) of the previous paper[1] is an excellent approximation to the energy distribution. The quantum yield of copper at photon energies where Eq. (60) is accurate is then

$$Y(\nu)=\int_{E_w}^{E_F+h\nu} C(E)\rho(E-\hbar\omega)dE \Big/ \int_{E_F}^{E_F+h\nu} \rho(E)\rho(E-\hbar\omega)dE. \quad (6)$$

Since the denominator of Eq. (6) is highly dependent on the density of states between the Fermi level and the vacuum level, comparison of the yield calculated using Eq. (6) and several trial density of states to the yield measured experimentally will give a measure of the density of states between the Fermi level and the vacuum level. The comparison of the measured yield and the calculated using Eq. (6) and the estimated density of states is shown in Fig. 15. The curves have been normalized for best fit.

The density of states derived from the trial and error methods described and used to calculate the curves shown in Figs. 13, 14, and 15 is shown in Fig. 16 and compared to the density of states calculated for copper by Burdick. The estimated accuracy in the experimentally determined density of states is $\pm 15\%$. A more detailed comparison of the $d$-band density of states determined here with that calculated by Burdick is given in Fig. 17.

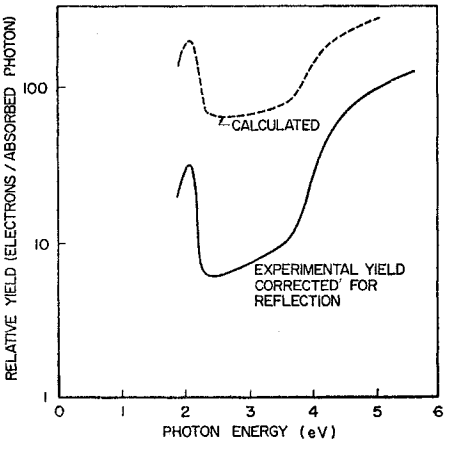


FIG. 15. Measured and calculated quantum yield for copper.

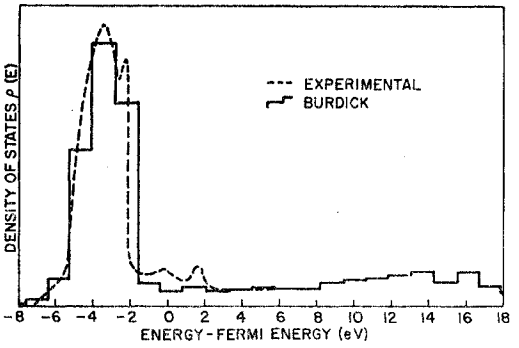


FIG. 16. Final estimate of the density of states in Cu. The dashed curve indicates the density determined experimentally. The solid curve is from the band calculation of Burdick (Ref. 6).

## G. The Effect of Electron-Electron Scattering

### *1. Lifetime Broadening*

One effect of electron-electron scattering in a solid is lifetime broadening.[20] In photoemission this produces broadening of peaks as the peaks are excited to higher energies. Figures 9 and 18, showing only the portion of electron energy distributions due to excitation of $d$-band electrons, illustrate the way the narrow peak near the top of the $d$ band is broadened due to this effect.

Information on the mean free path for electron-electron scattering can be gained from lifetime broadening effects. An estimate of the lifetime for scattering $\tau$ can be made by relating the broadening to the lifetime through the uncertainty principle. It is estimated that at approximately 6 eV above the Fermi level the peak near the top of the $d$ band is broadened to a width of 0.3 eV from a width at low energies of 0.2 eV. Assuming that the uncertainty in energy $\Delta E$ at this energy corresponds to 0.1 eV, the lifetime $\tau$ is given by[21]

$$\Delta E\tau=\hbar/2. \quad (7)$$

Using Eq. (7), the lifetime for scattering of an electron 6 eV above the Fermi level in copper is $3\times10^{-15}$ sec.

To obtain the mean free path for scattering, it is necessary to estimate the velocity. Since it is not practical to obtain the velocity from the actual band structure, it will be estimated using the free-electron model

[20] H. R. Philipp and H. Ehrenreich, Phys. Rev. 129, 1550 (1963).

[21] R. H. Dicke and J. P. Wittke, *Introduction to Quantum Mechanics* (Addison-Wesley Publishing Company, Inc., Reading, Massachusetts, 1960), p. 133.

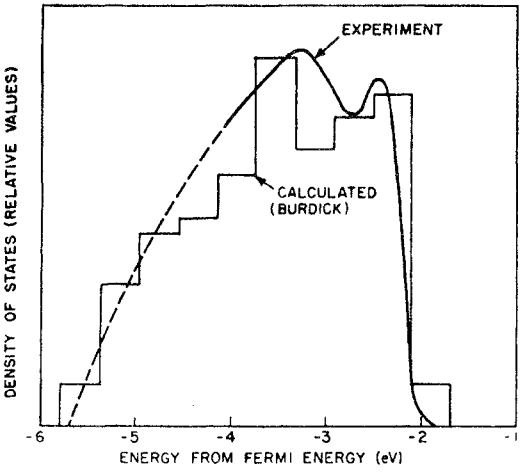


FIG. 17. Density of states of $d$ band of copper.

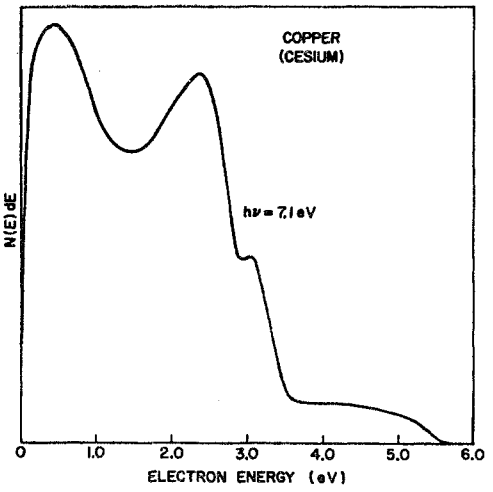


FIG. 19. Energy distribution of photoemitted electrons from copper—$h\nu = 7.1$ eV.

for a metal. The Fermi energy in copper is 7.0 eV,[22] so the group velocity $v_g$ of an electron 6 eV above the Fermi surface might be crudely estimated to be given by

$$E = e(6+7) = \tfrac{1}{2}mv_g^2. \quad (8)$$

Assuming the free electron mass, the velocity $v_g$ is $2.5\times10^8$ cm/sec. From the estimated lifetime and group velocity, the mean free path for electron-electron scattering in copper is 75 Å at 6 eV above the Fermi energy. This figure is in close agreement with measured mean free paths at similar energies in gold.[23]

### 2. *Contribution of Once-Scattered Electrons*

At photon energies greater than 6 eV, a low-energy peak appears in the energy distribution curves at a constant energy about 0.5 eV above the vacuum level as shown in Figs. 19 and 20. This peak is due to low-energy electrons produced by electron-electron scattering events. It is possible to gain a great deal of information on the electron-electron scattering process in copper by a study of such curves.

A theoretical expression for the energy distribution of photoemitted electrons including electron-electron scattering is given by Eq. (5). In order to use this expression and the density of states to predict the energy distributions, it is necessary to know the matrix element $M_s$ for the scattering probability in Eq. (33) of the previous paper.[1] Since the electron rules and wave functions involved in the scattering process are not well known, and since the Born approximation used in deriving Eq. (33) of the preceding paper may not be valid in metals such as copper and silver for the energy ranges of interest here,[24] it does not seem feasible at present to calculate the matrix element $M_s$; rather, an

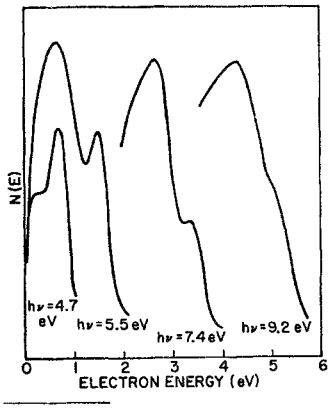


FIG. 18. Illustration of lifetime broadening in copper.

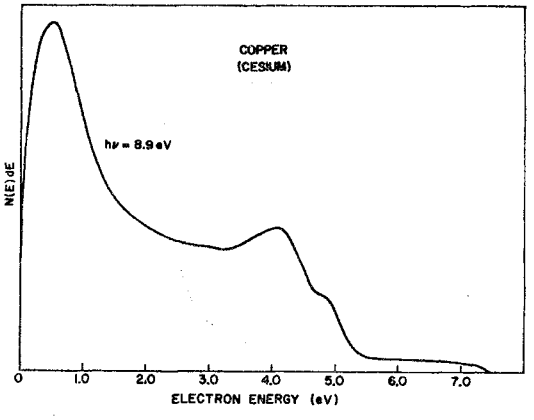


FIG. 20. Energy distribution of photoemitted electrons from copper—$h\nu = 8.9$ eV.

[22] A. J. Dekker, *Solid State Physics* (Prentice-Hall, Inc., Englewood Cliffs, New Jersey, 1957), p. 215.

[23] S. M. Sze, TR No. 1659-4, Contract AF 33(616)-7726, Stanford Electronics Laboratories, Stanford, California, April 1963 (unpublished); C. A. Mead, Phys. Rev. Letters 8, 56 (1962).

[24] K. Motizuki and M. Sparks, M.L.R. No. 1032, Contract SD-87 (ARPA), W. W. Hansen Laboratories of Physics, Stanford University, California, May 1963 (unpublished).

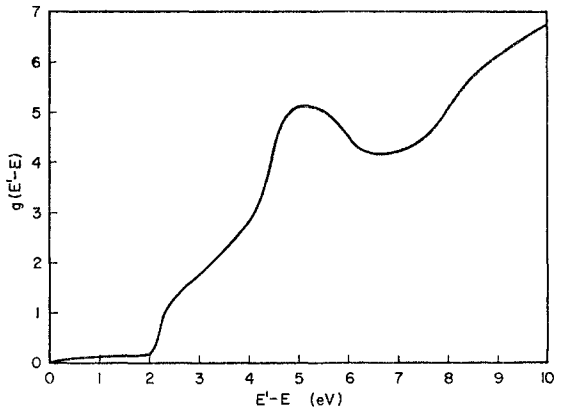


FIG. 21. Function $g(E'-E)$ for copper.

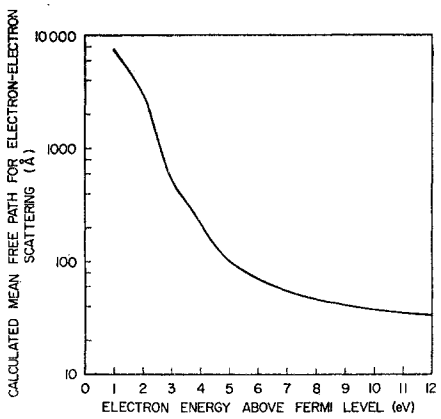


FIG. 23. Calculated mean free path for electron-electron scattering for copper.

approximation will be made which greatly simplifies the problem. This is that $M_s$ is a constant independent of the $k$ vector of the electrons involved in the scattering event.

Using a constant $M_s$ and the copper density of states determined in Sec. F, $g(E',E)$ and $P_s(E')$ have been calculated according to the following equations from the previous paper,[1] and are shown in Figs. 21 and 22.

$$g(E',E)=\frac{2\pi}{\hbar}|M_s|^2\int_0^\infty \rho(E_0)F(E_0)\rho(E_0+E'-E)\times[1-F(E_0+E'-E)]dE_0, \quad (9)$$

$$P_s(E')=\int_0^\infty p_s(E',E)dE. \quad (10)$$

The integrations required in the calculations were performed graphically using a compensating planimeter. Again, assuming a free electron group velocity $v_g$ given by

$$e(E+7)=\tfrac{1}{2}mv_g^2, \quad (11)$$

where $E$ is the electron energy above the Fermi level in eV and the Fermi energy in copper is 7 eV, the relative mean free path for electron-electron scattering has been calculated using

$$l(E)=v_g(E)/P_s(E) \quad (12)$$

and is shown in Fig. 23. The curve has been normalized to give a mean free path of 75 Å at 6 eV above the Fermi level in accord with the measurement of Mead[23] and Sze[23] in Au and the mean free path determined here by the lifetime broadening analysis. The accuracy of the curve is, of course, limited by the assumptions on which the calculation is based.

Using the values of $p_s(E')$, $P_s(E')$, $l(E)$ given in Figs. 21, 22, and 23, respectively, and the copper density of states given in Fig. 16, the energy distribution of photoemitted electrons was predicted according to Eq. (5) at photon energies of 7.5 and 11.0 eV. The compari-

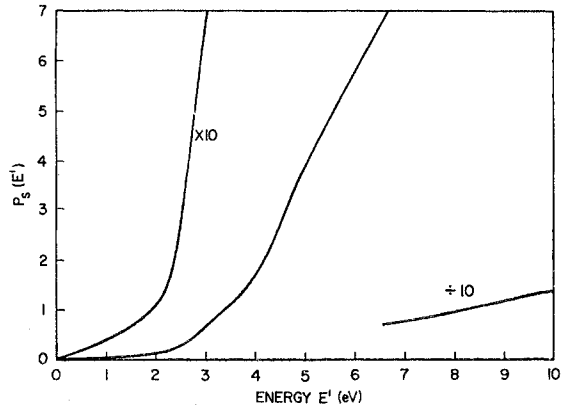


FIG. 22. Calculated $P_s(E')$ for copper.

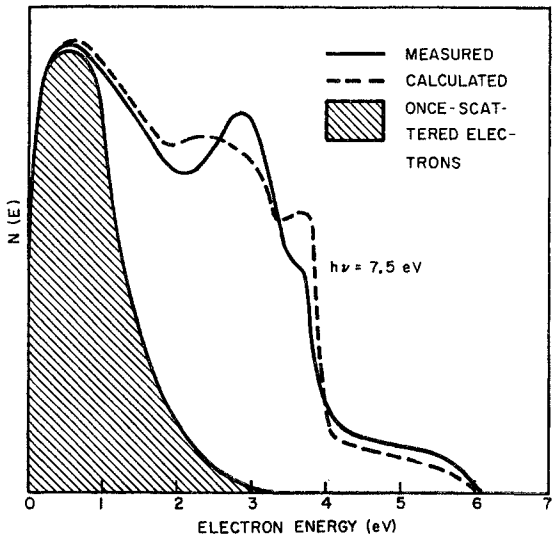


FIG. 24. Calculated and measured energy distribution of photoemitted electrons—$h\nu=7.5$ eV.

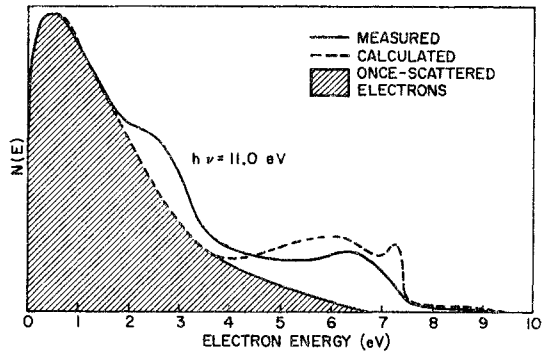


FIG. 25. Calculated and measured energy distribution of photoemitted electrons—$h\nu = 11.0$ eV.

sons between the predicted curves and the theoretical curves, normalized for best fit, are shown in Figs. 24 and 25. The contribution of once-scattered electrons to the curves is shown to illustrate the magnitude.

The good agreement between the calculated and the measured values of $N(E)$ verifies that the low-energy peak is due to scattered electrons, and that the assumptions of $v_g$ given by Eq. (11) and constant $M_s$ are reasonable first approximations. The disappointing feature of the results is that the theory fails to predict the structure appearing at about 3 eV above the vacuum level in the curve of $h\nu = 11.0$ eV. This failure is probably due to the fact that $M_s$ is not a constant; however, the possibility that this structure is due to additional structure in the density of states cannot be completely ruled out. The probability of this structure being due to additional energy bands seems small since there is no evidence of such structure in the calculated band structure.

Figure 26 shows energy distribution curves at photon energies where this peak occurs. It is evident that the peak moves to higher energies in increments equal to the increase in $h\nu$, and appears to be about 4 eV lower in energy than that part of the distribution due to excitation of $d$-band electrons. Referring to the density of states of copper shown in Fig. 16, the peak appearing in Fig. 26 may be due to electrons initially excited from the $d$ bands which scatter by exciting electrons at the top of the $d$ bands to the high density of states 1.8 eV above the Fermi level before escaping. The energy loss involved in this process is 4 eV, so a strong probability for this type of scattering would result in the observed behavior. The electron excited from the $d$ band by the scattering event may also escape, resulting in an increase in yield in this photon energy range. Such an increase is observed experimentally (see Fig. 2). If this is indeed the precess, it indicates that $M_s$ joining states near the top of the $d$ band and $X_4'$ is particularly strong.

### H. The Optical Constant, $\epsilon_2$, of Copper

The photoemission data have been used to obtain the density of states in Cu and to determine that nondirect transitions on the average make a stronger contribution to the results than direct transitions. By means of theoretical expressions derived for the photoemission process, the information on the density of states and the nature of the optically excited transitions has been used to predict the energy distributions at various photon energies and the spectral distribution of the quantum yield. The predicted values were found to be in good agreement with the measured values of these quantities. There may, however, be some question as to the validity of the conclusions and results obtained, particularly the conclusion that nondirect transitions are most important in copper. A legitimate question might also be raised as to whether or not the effects measured here and the density of states determined from the measurements are somehow peculiar to the photoemission experiment, even though experiments performed on other materials give no evidence of this.[25] In order to impose a much more severe test upon the results obtained here, these results will be used to calculate the relative value of $\epsilon_2$, the imaginary part of the dielectric constant, under the assumption that only nondirect transitions contribute significantly to optical absorption. This can then be compared to the independently measured $\epsilon_2$ and the two questions raised above can be answered. For $h\nu < 2$ eV, the optical constants of copper are dominated by the "free-electron" transitions and are not of interest here. However, for $h\nu > 2$ eV, the interband transitions dominate. It is this latter spectral region which will be of interest to us.

When nondirect transitions are dominant, the probability for an optical transition will depend on the product of the initial and final density of states. Neglecting lifetime broadening, the imaginary part of the dielectric constant, $\epsilon_2(\nu)$, will be given by

$$\epsilon_2(\nu) = \int_{E_F}^{E_F+h\nu} \frac{A\rho(E)\rho(E-h\nu)dE}{\nu^2}, \qquad (13)$$

where $E_F$ is the Fermi energy and $A$ contains the

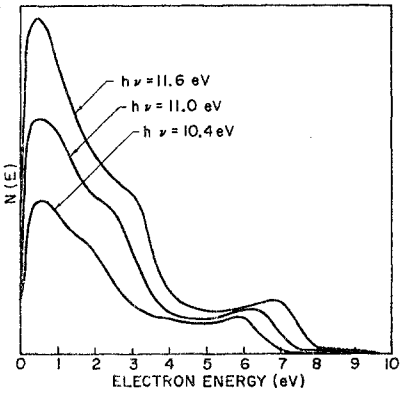


FIG. 26. Energy distribution of photoemitted electrons from copper—$h\nu > 10$ eV.

[25] W. E. Spicer and R. E. Simon, Phys. Rev. Letters 9, 385 (1962).

squared matrix element joining the initial and final states. The Fermi function at absolute zero temperature has been used in Eq. (13). This should give negligible error since $h\nu \gg kT$. Using Eq. (13), $\epsilon_2(\nu)$ may be calculated provided the density of states and the squared matrix element are known. Densities of states for copper have been obtained both from the photoemission data and from Burdick's theoretical calculation.[6] Since there is no simple method of determining the matrix element, $A$ in Eq. (13) will be assumed to be a constant. Although not correct in detail, such an assumption has been shown to be a good first approximation.[20]

Using Eq. (13) and the density of states given in Fig. 16, and assuming $A$ to be an energy-independent parameter determined empirically, $\epsilon_2(\nu)$ has been calculated. The curve obtained from the experimentally determined density of states as well as that obtained using the density of states calculated by Burdick are compared in Fig. 27 with $\epsilon_2(\nu)$ obtained by Kramers-Kronig analysis of the measured copper reflectance data by Ehrenreich and Philipp.[11] The curves were matched for best fit. Considering all of the possible sources of error, strikingly good agreement is obtained between the calculated and experimental curves of $\epsilon_2(\nu)$. The experimental peaks at 2.4 and 4.8 eV are reproduced in the curves calculated from the experimentally determined $\rho(E)$. These do not appear when Burdick's $\rho(E)$ is used and one should not expect these to appear since the histogram of the density of states calculated by Burdick involved an energy interval of 1.2 eV.

The two peaks appearing in $\epsilon_2$ in Fig. 27 should not be interpreted as being due to the two peaks in the $d$-band density of states. The energy separation of the peaks in $\epsilon_2$ is 2.4 eV, whereas the energy separation of the peaks in the $d$-band density of states is 0.9 eV. The peak at 2.4 eV in $\epsilon_2$ is due to the onset of transitions from the $d$ bands to states just above the Fermi level. The peak at 4.8 eV is due chiefly to transitions from the $d$ bands to the peak in the copper density of states at $X_4'$, 1.8 eV above the Fermi level.

Good agreement has been obtained between $\epsilon_2$ calculated from the experimentally determined density of states under the assumption of nondirect transitions and that measured experimentally. This agreement indicates that the optical transitions observed in the photoemission experiment are typical of optical transitions in copper and not somehow unique to the photoemission experiment. As an independent check of the results and conclusions drawn from the photoemission experiments, this agreement is particularly reassuring.

It is recognized that the interpretation of the optical data given here is different from that proposed previously.[11] The key point is the importance of nondirect transitions. In view of this it is, perhaps, worthwhile to compare the various interpretations in more detail. A detailed discussion will be made here only for Cu; however, similar arguments can be applied to Ag.

The first transition of importance in Cu is that at approximately 2.1 eV. This produces sharp rises in $\epsilon_2$ and $\sigma$.[26] The change in $\epsilon_2$ and $\sigma$ associated with this transition is greater than that associated with any other sharp interband transition. Through the critical point analysis,[11] this transition has been associated with a direct transition from states near $L_3$ in the calculated band structure to the Fermi level. However, due to the fact that $L_2'$ lies below the Fermi surface,[27] there is no critical point in the joint density of states associated with transitions from $L_3$ to the Fermi level. It is doubtful that such a large change in $\sigma$ and $\epsilon_2$ could occur (assuming only direct transitions) unless a critical point in the joint density of states existed. If nondirect transitions are assumed, this difficulty disappears, the 2.1 eV structure appears in a natural way, and its strength is seen to be due to the transitions from the very high density of initial states located near the edge of the $d$-like bands to the continuum of states above the Fermi level.

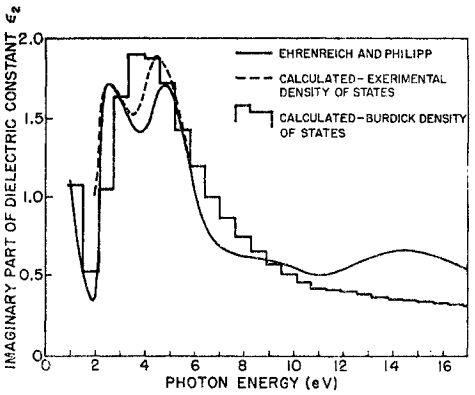


FIG. 27. Imaginary part of the dielectric constant $\epsilon_2$ for copper.

The next structure appears at about 4.8 eV. According to the critical point analysis, this is due to the critical point in the joint density of states involving transitions from $X_5$ to $X_4'$. If this were the case the absorption should appear at a photon energy equal to the energy separation between $X_5$ and $X_4'$. Both the band calculations and the photoemission measurements set this separation at approximately 4 eV. According to the analysis in this paper, the peak at 4.8 eV is due to transitions from the $d$ band to the high density of states associated with the $X_4'$ point. Since the maximum in the $d$-band density of states lies about 1 eV below $X_5$, the peak in $\epsilon_2$ should be expected to occur at about 5 eV as indeed it does.

---

[26] This discussion will be restricted to $\sigma$ and $\epsilon_2$ since these quantities are directly proportional to optical transition probabilities and can be related directly to the band structure. It is not as useful to examine the absorption coefficient $\alpha$ since it depends on both $\epsilon_1$ and $\epsilon_2$ and cannot be related in a simple manner to the band structure.

[27] This has been well verified by de Haas–van Alphen measurements and is in agreement with the photoemission measurements reported here.

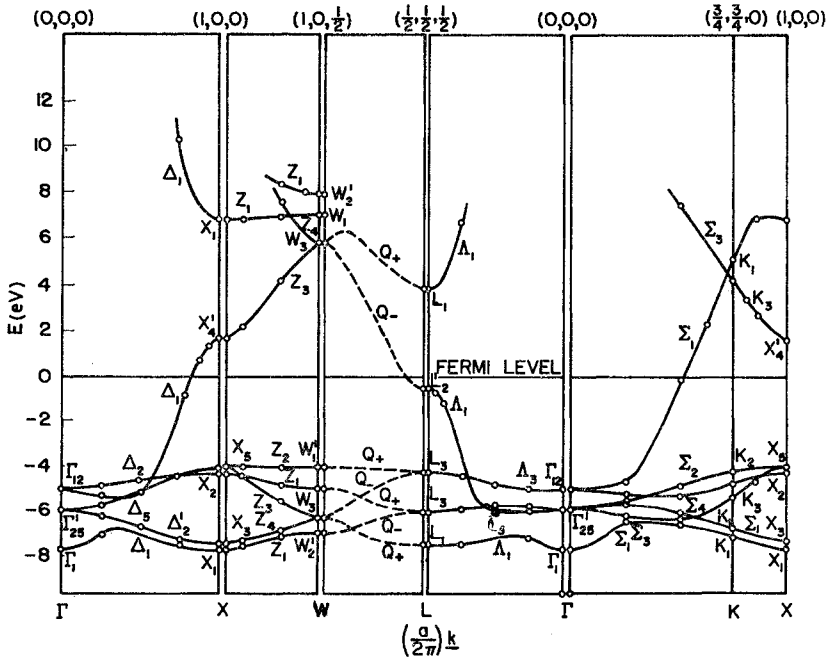


FIG. 28. Calculated band structure of silver after Segall (Ref. 5).

In the critical point analysis, the $L_2'$ to $L_1$ transition is also associated with the peak near 5 eV. However, it is not immediately clear whether or not this transition would make a strong contribution to $\epsilon_2$ or $\sigma$.[20] In the photoemission measurements the direct transition from $L_2'$ to $L_1$ is clearly seen. However, the relative strength of such a transition is found to be quite small.

It is interesting to compare the application of the critical-point analysis to Ni with that to Cu. In the band structure proposed by Ehrenreich, Philipp, and Olechna for Ni,[28] $L_2'$ as well as unfilled $d$-like bands lie above the Fermi surface and the filled $L_3$ band lies 1.7 eV below the Fermi surface. Therefore, according to the critical point analysis, a much stronger transition should occur from the filled band at $L_3$ to states near the Fermi surface in Ni than in Cu. However, the converse occurs. Only relatively weak structure is seen in Ni near 1.7 eV.[29] If the background absorption is subtracted out, the $\Delta\sigma$ associated with that transition in Ni is approximately one-fourth as great as that associated with the $L_3$ to Fermi level transition in Cu. On the basis of nondirect transitions, it may be possible to explain this behavior.

It would appear that in Cu and Ag the major features of $\epsilon_2$ or $\sigma$ as well as the photoemission data can be explained much more satisfactorily in terms of nondirect transitions than in terms of critical point analyses based on the assumption that only direct transitions are important. The one remaining unknown is that concerning the strength of the matrix elements. Based on past experience, it seems unlikely that any large changes in the conclusion of this paper will be produced by detailed calculations of matrix elements; however, it is important that these calculations be made in order to remove the single remaining question.

## III. PHOTOEMISSION FROM SILVER

### A. The Calculated Band Structure of Silver

The band structure of silver is somewhat more difficult to calculate accurately than that of copper. Due to the fact that silver is a heavier atom, the use of nonrelativistic atomic wave functions and the potential based on them will lead to more error.

Segall[30] has calculated the band structure of silver ignoring relativistic effects using two different potentials. The first was determined from the free ion $Ag^+$ Hartree functions in the same manner as that for copper, and the second used the Hartree-Fock free-ion function. The results for the two fairly different potentials were not too dissimilar, their main difference being that the $d$ bands were located in different positions $-2.2$ and 5.2 eV below the Fermi level for the Hartree and the Hartree-Fock methods, respectively. This is not surprising since it is well known that the Hartree-Fock orbitals are more tightly bound than the Hartree functions. The band structure above and just below the Fermi level was very similar for the two calculations.

[28] H. Ehrenreich, H. R. Philipp, and D. J. Olechna, Phys. Rev. 131, 2469 (1963).

[29] See Fig. 2 of Ref. 28.

[30] B. Segall, Report No. 61-RL-(2785G), General Electric Research Laboratory, Schenectady, New York, July 1961 (unpublished).

From the calculations, Segall concluded that the band structure of silver was relatively insensitive to the details of the potential used for the calculation. Knowing that the $d$ bands are located in silver about 4 eV below the Fermi level, he suggested that the $d$ bands be simply shifted in an *ad hoc* way to their proper location, and that all other features of the band structure be assumed correct. The resulting band structure is shown in Fig. 28.

### B. The Quantum Yield

Comparing the band structure of silver in Fig. 28 to that of copper in Fig. 1, the only major difference appears to be in the location of the $d$ bands. For this reason, very similar results in the quantum yield curves of copper and silver might be expected. The spectral distribution of the quantum yield of silver with cesium on the surface is shown in Fig. 29. Referring to the copper and silver yields in Fig. 3 and 29 some similarity is seen to exist between the curves if allowance is made for the fact that the yield decrease at $h\nu=2.1$ eV and increase at $h\nu=3.7$ eV in copper should correspond to a yield decrease at $h\nu=4$ eV and increase at $h\nu=5.6$ eV in silver because the $d$ bands of silver are approximately 2 eV deeper. However, in silver there is not the range of low yield between the onset of $d$-band absorption and the onset of photoemission due to $d$-band electrons being excited to states above the vacuum level. Rather, the quantum yield of silver goes through a sharp minimum at $h\nu=3.85$ eV. This suggests that there is an additional, strong source of photoelectrons in Ag with a threshold at approximately 4 eV. It will be shown in Sec. D that this additional process is the Auger process. When the photon energy becomes large enough to excite electrons from the silver $d$ bands (approximately 4 eV), the holes left behind take part in a strong Auger process resulting in electrons being excited to states above the vacuum level. This causes the increase in quantum yield at approximately 4 eV in silver. It also causes the increase in silver yield at 5.6 eV, where $d$-band electrons

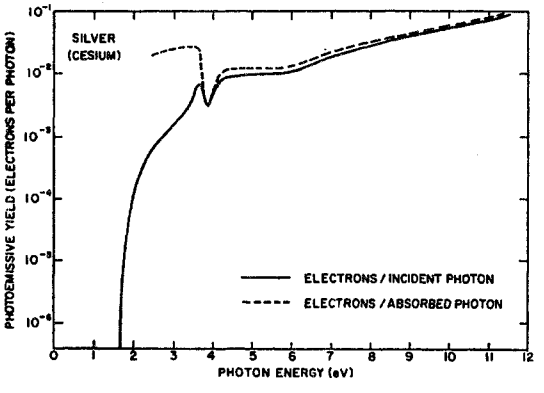


FIG. 29. Quantum yield of silver.

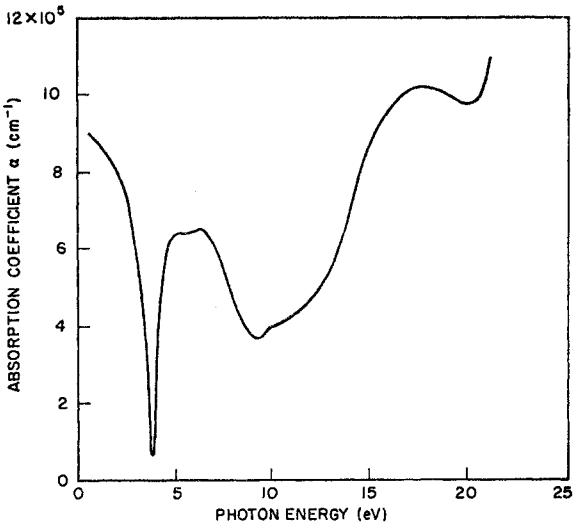


FIG. 30. Absorption coefficient $\alpha$ for silver, after Ehrenreich and Philipp (Ref. 11).

are beginning to be excited to states above the vacuum level to be less pronounced than in copper.

From the preceding discussion, the yield minimum in silver at $h\nu=3.85$ eV can be explained as a decrease in yield due to the onset of $d$-band absorption followed by an increase in yield due to the Auger process. However, the fact that the yield minimum occurs at a photon energy corresponding to the strong plasma resonance in silver[11] suggests that there may be more factors involved. One effect of this resonance is shown in Fig. 30 where the silver absorption coefficient is plotted. Referring to Eq. (5), if the absorption coefficient becomes smaller than $1/l$, the yield will decrease since the electrons are excited deeper in the metal and they must travel further to reach the photoemitting surface. Hence, this effect may be responsible in part for the yield minimum in silver at $h\nu=3.85$ eV. Another effect of the resonance is that photons with energy near 3.85 eV may be absorbed in exciting plasma oscillations, thus not directly producing photoelectrons. This effect is discussed in Sec. J.

The quantum yield near threshold of silver with cesium on the surface can be used to determine the work function in a manner similar to that used for copper. Figure 31 shows the square root of the yield versus photon energy. The figure gives a work function for silver with cesium on the surface of 1.65 eV.

### C. Energy Distribution of Photoemitted Electrons—$h\nu<3.5$ eV

It has been pointed out in a previous section, and described in detail by Ehrenreich and Philipp,[11] that interband transitions do not become dominant in silver until $h\nu>3.5$ eV and that "free-electron" absorption is dominant for $h\nu<3.5$ eV. The energy distribution of photoemitted electrons from silver for $h\nu<3.5$ eV shown

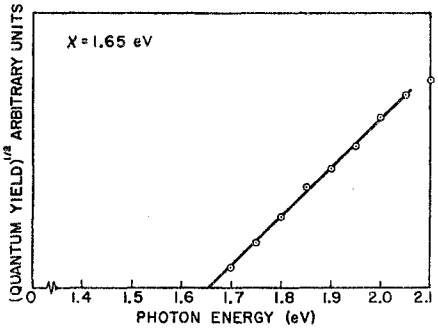


FIG. 31. Evaluation of work function of silver with cesium on the surface.

in Fig. 32 demonstrates this. A peak near the maximum electron energy becomes more apparent as $h\nu$ increases, but does not dominate the distribution. This peak is due to nondirect transitions from the peak in the density of states at $L_2'$ in the calculated band structure (Fig. 28). The remainder of the distributions is the characteristic "free" electron contribution.

The peak near the maximum electron energy for $h\nu<3.5$ eV follows the relation

$$E=h\nu-1.95\text{ eV}, \tag{14}$$

where $E$ is the energy of the peak with respect to the vacuum level. Since the work function of silver is 1.65 eV, the peak in the energy distributions is due to a peak in the density of states at $L_2'$ located 0.3 eV below the Fermi level. Figure 32 indicates that a larger peak in the density of states is associated with symmetry point $L_2'$ in silver than in copper.

In the photoemission data of silver, there is no evidence of a peak in the density of states at $X_4'$, 1.8 eV above the Fermi level, as found in copper. This might be the result of a smaller density of states associated with $X_4'$ in silver, or of the $X_4'$ symmetry point being located at a lower energy so that the peak was masked by the threshold function. In Sec. G, $\epsilon_2(\nu)$ for silver is calculated based on the assumption that there is no strong peak in the density of states above the Fermi level. The calculated $\epsilon_2(\nu)$ is in reasonable agreement with the measured values. Thus, it is most likely that the former is true, although the possibility that $X_4'$ lies a few tenths of an electron volt above the Fermi level cannot be ruled out.

### D. Evidence of the Auger Process

The Auger process has been considered theoretically by several authors,[31] and its effect on photoemission data has been discussed in the previous paper. If the density of states of silver is known, an estimate of the effect of the Auger process can be made using Eqs. (48) and (49) of the previous paper. However, due to the peculiarity of the density of states of silver, an approximation can be made which greatly simplifies the analysis.

In silver, the $d$ bands produce a very high density of states which extends approximately from 4 to 7 eV below the Fermi level (see Fig. 28). As a first approximation, it will be assumed that the only holes that take part in the Auger process are those located at the top of the $d$ bands. (Reasons why this is a good approximation will be given later.) Under this assumption, there will be no evidence of an Auger effect in the photoemission data until the photon energy is large enough to excite $d$-band electrons ($h\nu>3.8$ eV). In addition, for photon energies greater than 3.8 eV, the effect of the Auger process on the energy distribution of the photoemitted electrons will be independent of photon energy since the holes involved will always lie at the top of the $d$ band.

Except for the peak in the silver density of states 0.3 eV below the Fermi level, the density of states in silver above the $d$ bands is found to be approximately constant. This will be established in later sections. If the density of states of silver is assumed a constant, $\rho_0$, above the $d$ bands, and the matrix element $M_a$ is assumed energy-independent, $p_a(E_0,E)dE$ in Eq. (44) of the previous paper can be evaluated

$$p_a(E_0,E)dE=(2\pi/\hbar)|M_a|^2\rho_0{}^3[(E_F-E_0)-(E-E_F)]dE$$
$$0<(E-E_F)<(E_F-E_0). \tag{15}$$

In Eq. (15) the Fermi function at absolute zero temperature has been used. Since only the holes at the top of the silver $d$ band (approximately 4 eV below the Fermi level) are being considered, Eq. (15) becomes

$$p_a(E)dE=(2\pi/\hbar)|M_a|^2\rho_0{}^3[4-(E-E_F)]dE$$
$$0<(E-E_F)<4\text{ eV}, \tag{16}$$

where the energies are measured in electron volts.

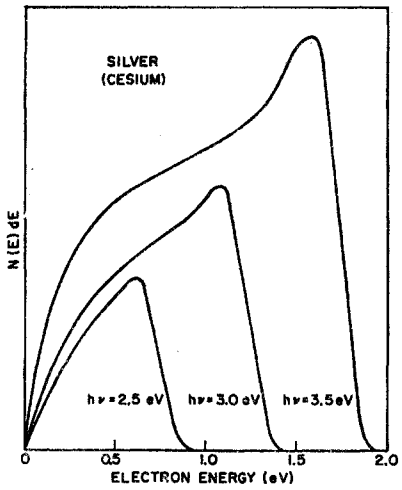


FIG. 32. Energy distribution of photoemitted electrons from silver—$h\nu<3.5$ eV.

[31] See, for instance, H. D. Hagstrum, Phys. Rev. 96, 336 (1954).

Substituting Eq. (16) in Eq. (49) of the previous paper gives for the contribution of the Auger process to the energy distribution of photoemitted electrons

$$N_a(E)dE \propto \frac{KC(E)}{\alpha+[1/l(E)]}[4-(E-E_F)]dE$$

$$0<(E-E_F)<4 \text{ eV}. \quad (17)$$

This contribution is plotted in Fig. 33, assuming a reasonable threshold function and using the work function of 1.65 eV for silver.

Holes located at other energies than the top of the $d$ bands should have negligible effect on the distribution shown in Fig. 33. Holes between the $d$ bands and the Fermi level can be neglected because the density of states is smaller and because fewer Auger electrons excited by these holes can achieve energy greater than threshold. Holes produced deeper in the $d$ bands will likely relax through the Auger process to the top of the $d$ bands, the energy exchange involved generally being too small to excite any electrons to states above the vacuum level.

Figure 33 indicates that the Auger process will result in an energy distribution of electrons decreasing with energy to a maximum energy of approximately 2.4 eV above the vacuum level. Figure 34 shows the experimentally determined energy distribution curves for silver for photon energies of 4.1, 4.3, 4.8, and 5.4 eV. The distributions have been normalized to coincide at low energies. Figure 35 shows the energy distributions at photon energies of 3.6, 3.8, and 4.0 eV. Except for the high-energy peak associated previously with a peak in the density of states 0.3 eV below the Fermi level, the energy distributions shown in Figs. 34 and 35 are very similar to the distributions predicted on the simple model of the Auger process. A low-energy peak due to the Auger process begins to appear when the photon energy is approximately 4 eV, and at higher photon energies the distribution is essentially independent of photon energy.

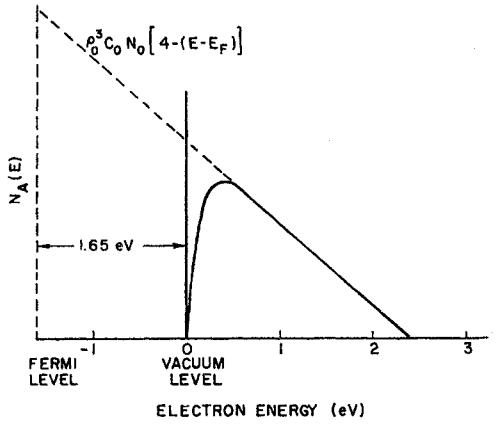


FIG. 33. Energy distribution of photoemitted electrons to be expected due to Auger process.

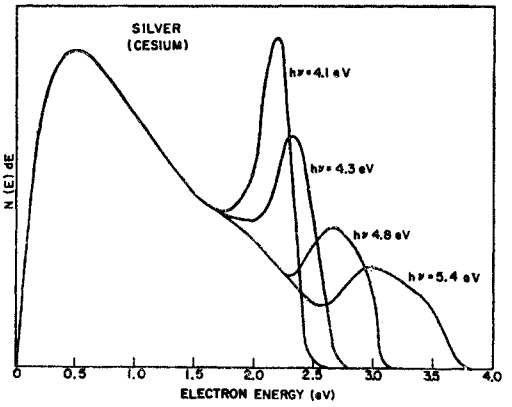


FIG. 34. Energy distribution of photoemitted electrons from silver—$h\nu$=4.1 to 5.4 eV.

By extrapolation, the maximum energy of the Auger photoelectrons is found to be 2.5 eV independent of photon energy.

The energy distribution produced by the Auger effect has certain characteristics which allow it to be distinguished from the energy distribution characteristic of inelastically scattered electrons with which it might be confused. To the first approximation, the probability of Auger emission will be proportional to the probability of a hole being produced by optical absorption in the $d$ band. In Ag the probability increases very sharply from zero to a large, approximately constant value within a few tenths of an electron volt of the threshold (about 4 eV) for $d$-band absorption.[11] As a result the characteristic distribution of electrons due to Auger electrons should appear abruptly for photon energies near 4.0 eV and should be relatively constant in shape and magnitude from about 4.2 eV until $d$ electrons are excited directly into the distribution (at about 5.8 eV), obscuring the Auger distribution. As can be seen in Figs. 34, 35, and 37, such behavior is observed experimentally. The situation with Auger electrons is to be contrasted with that of a "slow" distribution produced by inelastic scattering. In the latter case, the number of inelastically scattered electrons increases relatively slowly and monotonically as the photon energy increases (see Figs. 8, 19, 20, 23, and 24, and Refs. 23, 24, and 32) instead of appearing abruptly and then remaining constant over a large range in photon energy.

A possible explanation of the broad peak in Fig. 34 located between 1.5 and 2.5 eV involves the maximum in the density of states at $L_2'$. Because of this maximum, a probable event is for electrons near $L_2'$ to recombine with holes at the top of the $d$ band, energy being given up to neighboring electrons also near $L_2'$. The energies are such that this Auger process will result in a peak approximately 1.8 eV above the vacuum level as observed.

[32] J. J. Quinn, Phys. Rev. **126**, 1453 (1962).

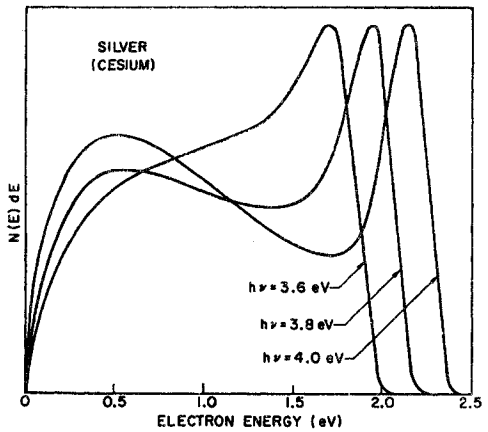


FIG. 35. Energy distribution of photoemitted electrons from silver—$\nu$ near the plasma frequency.

This simple model for the Auger process also explains why the process is negligible in copper. Since the $d$ bands in copper are only 2 eV below the Fermi level, a negligible fraction of the Auger-excited electrons are excited to energies above the vacuum level.

## E. Nondirect and Direct Transitions in Silver

The high-energy peak in the electron energy distributions in Fig. 34 exhibits the same behavior as that noted for the similar peak in copper. At a photon energy of approximately 4.1 eV the peak is a maximum, and at higher photon energies it splits into two peaks. One of the peaks moves to higher energy in increments equal to the change in photon energy, while the other moves to higher energy at a somewhat slower rate. The amplitudes of the peaks get smaller as the peaks are excited to higher energies because of strong energy-dependent electron-electron scattering.

The peaks in the energy distributions can be explained in terms of direct and nondirect transitions in the same way as the similar peaks were explained in copper. Figure 36 shows the energy of the initial states responsible for the largest peak in the distributions of Fig. 34 plotted versus $h\nu$. For photon energies less than 3.5 eV this peak is due to nondirect transitions from the peak in the density of states at $L_2'$. From the figure, it is evident $L_2'$ is located 0.3 eV below the Fermi level. At $h\nu=3.5$ eV, the direct transition is beginning to contribute. The initial states involved in the direct transition lie above $L_2'$ for $3.5<h\nu<4.2$ eV. As a result, the curve in Fig. 36 goes through a maximum at $h\nu=4.0$ eV. At $h\nu=4.2$ eV, the transition is occurring again from initial states at $L_2'$, 0.3 eV below the Fermi level. For $h\nu>4.2$ eV the initial state lies below $L_2'$. Since the peak at $h\nu=4.2$ eV is due to direct transitions from $L_2'$ to $L_1$, $L_1$ is located 3.9 eV above the Fermi level.

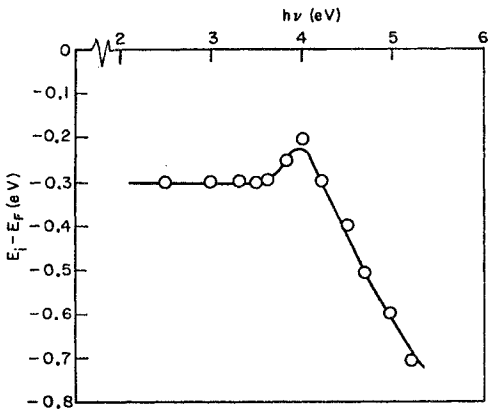


FIG. 36. Energy of initial states responsible for high-energy peak in photoemission data. The break at $h\nu=3.5$ eV is due to the onset of direct transitions.

## F. Transitions from the $d$ Bands

Since the $d$ bands in silver are located approximately 4 eV below the Fermi level, at photon energies greater than 5.7-eV $d$ bands electrons should be excited to states above the vacuum level. Figure 37 shows the electron energy distributions from silver for photon energies of 5.7 and 6.3 eV. At 5.7 eV there is no longer evidence of $d$-band electrons in the distribution, but at 6.3 eV a low-energy peak appears which is due to transitions from the $d$ bands. The energy distributions at $h\nu=7.8$ and 8.4 eV are shown in Figs. 38 and 39. The narrow peak in the distributions is due to a peak in the $d$-band density of states, and the peak following the first peak at approximately 1 eV lower energy is also due to the $d$ bands. The lowest energy peak appearing in the curve at $h\nu=7.8$ eV and more strongly in the curve at $h\nu=8.4$ eV is due to scattered electrons.

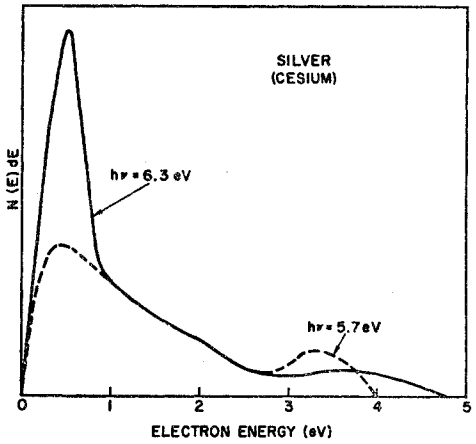


FIG. 37. Energy distribution of photoemitted electrons from silver—$h\nu=5.7$ eV, 6.3 eV.

By a method identical to that used for copper, it can be shown that optical transitions from the $d$ bands in silver are nondirect. The shape of the $d$-band distri-

bution in the experimental curves is unchanged as photon energy is increased except for a distortion due to scattering. The peaks in the distributions move to higher energies in increments equal to the change in photon energy. For this reason, features of the $d$-band density of states can be determined from Figs. 37–39. It is found that the $d$ bands in silver are located 3.75 eV below the Fermi level. There are at least two peaks in the density of states, one about 0.3 eV wide located 4.1 eV below the Fermi level, and the other about 1.2 eV wide located approximately 5.3 eV below the Fermi level. The exact location and width of the second peak cannot be determined exactly because of the masking due to scattered electrons. When the magnitude of the scattering peak is estimated using Eq. (5) and subtracted from the distributions shown in Figs. 38 and 39, there is no evidence of further structure in the $d$ bands. Because of this, it is likely that the silver $d$-band density of states consists of only the two peaks mentioned above.

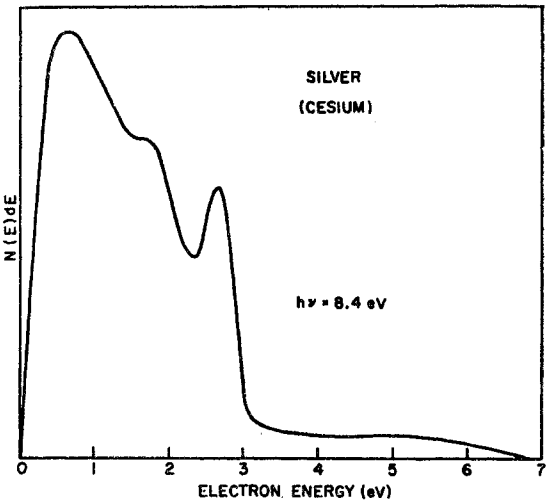


FIG. 39. Energy distribution of photoemitted electrons from silver—$h\nu = 8.4$ eV.

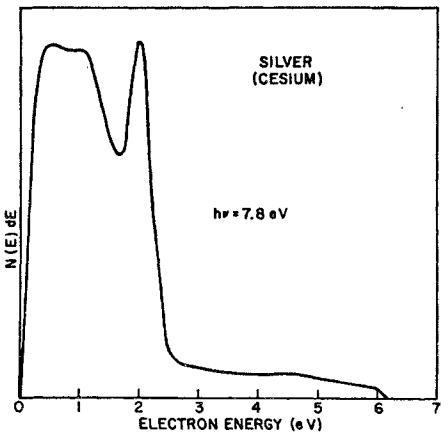


FIG. 38. Energy distribution of photoemitted electrons from silver—$h\nu = 7.8$ eV.

## G. The Silver Density of States

The density of states of silver is considerably more difficult to determine exactly from the photoemission data than that of copper. At photon energies less than 3.5 eV, the electron energy distributions are dominated by the "free electron" transitions; at photon energies between 3.8 and 6.5 eV, the distributions are dominated by the Auger effect; and at photon energies above 7.0 eV, the distributions are distorted badly due to scattering. However, several important features of the density of states can be determined. The location and density of states of part of the $d$ band can be estimated, and two peaks in the density of states identified. The only other evidence of structure in the density of states is the peak at $L_2'$ 0.3 eV below the Fermi level. From these considerations, a silver density of states has been estimated and is shown in Fig. 40. The accuracy of the density of states in Fig. 40 is not as good as that for copper. However, the general features are correct as indicated in Fig. 41 where the imaginary part of the dielectric constant has been calculated and compared to the measured values. The curve was calculated by the same method used for copper.

It is significant that only one strong peak occurs in the experimental and the calculated $\epsilon_2$ curves in Ag, whereas two appear in Cu. This is further evidence that Ag lacks a strong maximum in the density of states corresponding to that detected in Cu 1.8 eV above the Fermi level ($X_4'$).

## H. The Threshold Function $C(E)$ for Silver

Because of the relatively constant density of states in silver above the Fermi level and the accuracy with which it was possible to predict the electron energy distributions due to the Auger process, the threshold function $C(E)$ can be easily estimated. Figure 42 shows the measured energy distribution of photoemitted electrons at a photon energy of 4.8 eV. If the threshold function is essentially constant at energies more than 1 eV above

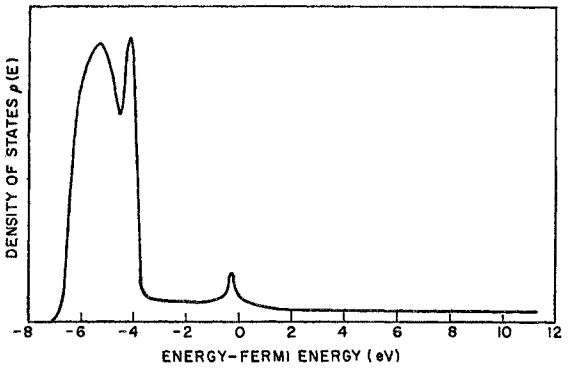


FIG. 40. Estimated density of states for silver.

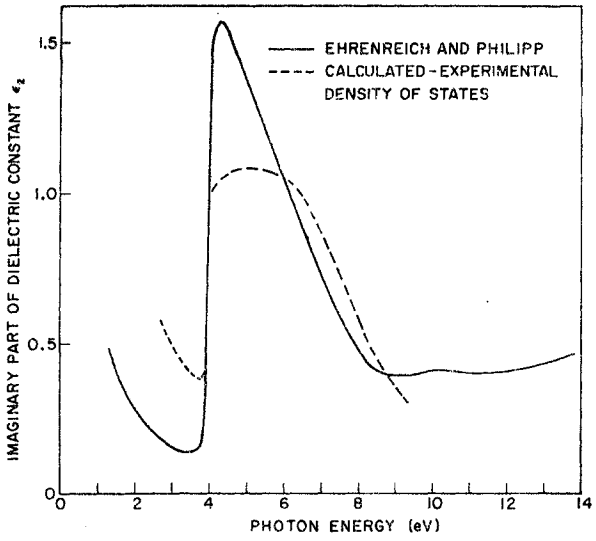


FIG. 41. Imaginary part of the dielectric constant $\epsilon_2$ for silver.

the vacuum level, the threshold function $C(E)$ must be proportional to the ratio between the measured energy distribution curve and the straight-line extrapolation of the Auger distribution to lower energies shown dotted in Fig. 42. The threshold function determined in this way is shown in Fig. 43. This is the threshold function that has been used with the copper data.

## I. The Effect of Electron-Electron Scattering

Electron-electron scattering in silver affects the photoemission data in a similar way to that in copper. Figure 34 shows that the high-energy peak in the energy distribution is reduced in size as the peak is excited to higher energy, but the quantum yield in this photon energy range is relatively constant. One would expect that, since direct transitions are beginning to occur, the height of the peak should increase rather than decrease. The observed behavior is due to the fact that the mean free path is a decreasing function of energy, and the probability of escape without scattering of a high-energy electron is correspondingly smaller than that of a lower energy electron. Figures 38 and 39 show the low-energy peak in the energy distribution which is due to the scattering of high-energy electrons. Figures 44 and 45 are the energy distributions of photoemitted electrons from silver at photon energies of 9.3, 10.5, and 11.4 eV, and show the lifetime broadening of the high-energy $d$-band peak (labeled $C$).

The mean free path at one energy can be estimated from the lifetime broadening of the sharp $d$-band peak in silver. This has been done in the same way as was done for copper in Sec. IIG1 but using a Fermi energy of 5.5 eV.[22] The estimated mean free path for electron-electron scattering at 5.5 eV above the Fermi level is 70 Å.

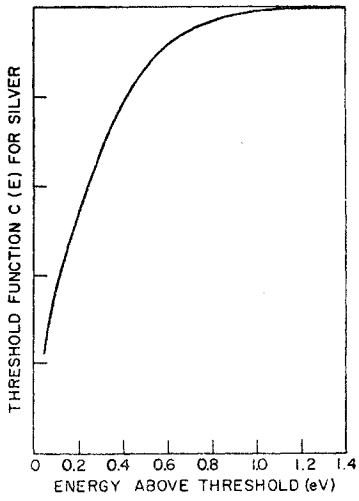


FIG. 43. Threshold function $C(E)$ for silver.

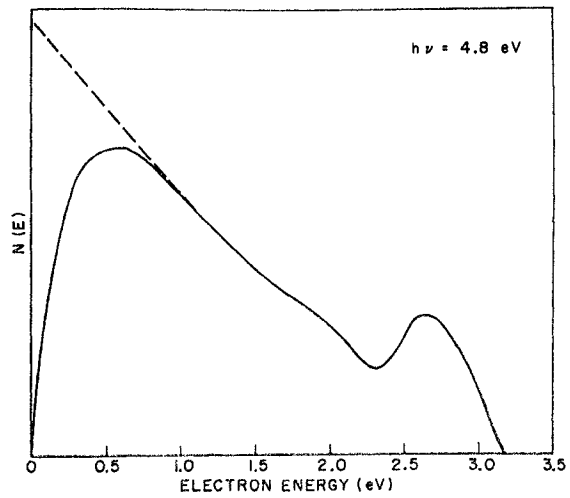


FIG. 42. Evaluation of threshold function $C(E)$ for silver.

Since it was not possible to determine the density of states in silver with the accuracy achieved with copper, no detailed calculations of $l(E)$, $p_s(E',E)$, and $P_s(E')$ were carried out. However, several of the important features of the scattering processes and their effect on the energy distribution of photoemitted electrons can be described without detailed calculations.

There is a high density of states in silver in the $d$ band approximately 4 eV below the Fermi level. When electrons have enough energy to scatter with these $d$ electrons and excite them to states above the Fermi level, there will be a large probability for scattering (short electron-electron mean free path). Referring to Fig. 34, it can be seen that strong scattering begins to reduce the size of the high-energy peak in the energy distribution curves when the peak corresponds to electron energies more than 2.3 eV above the vacuum level, or 3.95 eV above the Fermi level. This is in close agreement with the simple argument. In addition, since the

density of states in silver is relatively constant above the Fermi level, no structure in the scattering peak similar to that appearing in Fig. 26 for copper is to be expected, and none is observed (see Fig. 45).

### J. Effect of the Plasma Resonance at $h\nu = 3.85$ eV

The plasma frequency at $h\nu = 3.85$ eV in silver might affect the photoemission data in several ways. The decrease in yield at incident light frequencies near the plasma frequency which can be brought about by a decrease in the absorption coefficient has already been described. It might be expected that a further decrease in yield would result if an appreciable number of photons were absorbed producing plasma oscillations. However, if photoelectrons are produced by the relaxation of these plasma oscillations, the yield would not be reduced.

A further effect of the plasma resonance in silver has been mentioned in the previous paper.[1] Energetic electrons may lose energy in travelling through the metal by exciting plasma oscillations. In this scattering mechanism, the energy loss per scattering event is approximately equal to the energy corresponding to the plasma frequency. Hence, if this scattering process were strong in silver there would be a large probability of a scattering event with an energy loss of 3.85 eV. In the photoemission data, this would result, for instance, in a strong scattered peak in the energy distribution curves following by 3.85 eV the sharp peak in the distributions due to optical excitation of electrons from the top of the $d$ band. Since no such structure is observed in the energy distribution curves of silver, it is concluded that scattering of electrons by the creation of the 3.85-eV plasma oscillations in Ag is a weak scattering process compared to electron-electron scattering over the range of electron energy studied. This conclusion is in agreement with the theoretical results of Quinn.[32]

## IV. DISCUSSION AND CONCLUSIONS

One of the most significant features of the experimental results is the evidence that nondirect optically excited transitions are dominant in copper and silver. For transitions from the $s$- and $p$-like bands just below the Fermi level, this behavior is not unexpected since these transitions are the same as the "free carrier" transitions referred to in the literature.[11] Moreover, when the photon energy is such that a strong direct transition should occur from the $p$- and $s$-like states below the Fermi level, direct transitions are observed but it is found that the direct transitions are not as strong as the nondirect transitions. No evidence is found for direct transitions from the $d$ bands; only nondirect transitions are observed.

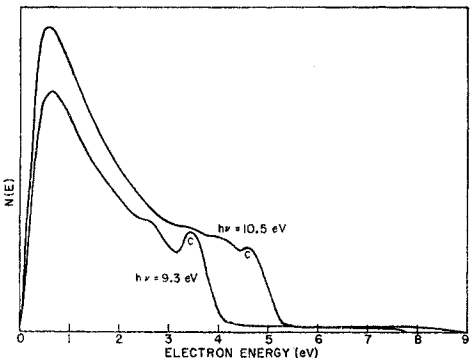


FIG. 44. Energy distribution of photoemitted electrons from silver—$h\nu > 9$ eV.

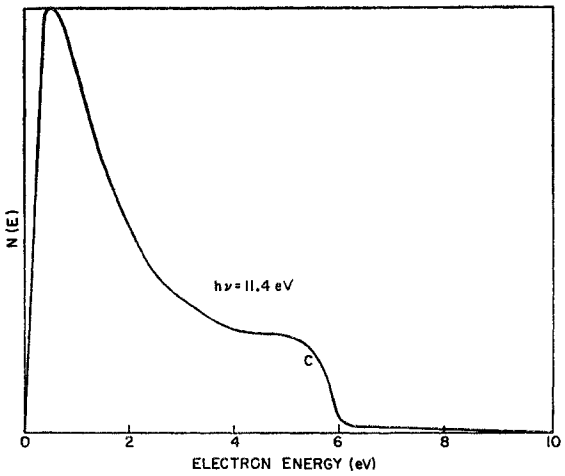


FIG. 45. Energy distribution of photoemitted electrons from silver—$h\nu = 11.4$ eV.

There are several possible explanations for the observed behavior. The second order transition probability involving phonons may be large enough in the metals to result in indirect transitions being stronger than direct transitions. This may occur even if the second-order matrix element is smaller than the first-order matrix element because of the larger number of electrons available to take part in phonon-assisted transitions. However, measurements of the quantum yield per incident photon of a copper phototube from threshold to $h\nu = 3.5$ eV at room temperature and at 77°K showed no noticeable difference in yield.

Another possible explanation for the observations is that a large probability exists for some other mechanism such as defects[34] to conserve $\bar{k}$ vector. This mechanism would not be expected to have a strong temperature dependence in agreement with the yield measurements at room temperature and at 77°K, and it might result in an increased "free" carrier absorption; however, it is difficult to see why it should force all $d$-band transitions to go via nondirect processes, whereas both direct

[33] D. L. Dexter, *Photoconductivity Conference*, edited by R. G. Breckenridge and B. R. Russel (John Wiley & Sons, Inc., New York, 1956), p. 155.

[34] C. Herring, in *Proceedings of the International Conference on Semiconductor Physics, Prague, 1960* (Publishing House of the Czechoslovak Academy of Sciences, Prague, 1960) p. 1044.

and nondirect transitions are observed in transitions between $p$- and $s$-like bands.

There is the additional possibility that the Bloch-wave representation of some of the electronic states in copper and silver may not be adequate.[34,35] In particular, this may be true for the $d$-band states because of the fact that no evidence of direct transitions from the $d$ bands was found and because the strong correlation effects in this band would tend to break down the one-electron approximation. This possibility cannot be ruled out on the basis of the close apparent agreement between the measured density of states and that calculated assuming Bloch-wave solutions for the wave equation.[6] This agreement might be accidental or it might have occurred because of the potential used in the calculation. It is clear that the density of states determined here are not in agreement with those obtained in earlier band calculations.[36]

By means of photoemission, the density of states has been determined in Ag and Cu and certain symmetry points in the $s$- and $p$-like bands have been located absolutely in energy. The experimental results of the photoemission study can be used to compare the metals copper and silver. It has already been mentioned that nondirect transitions are most important in both metals. The band structure and density of states of both are very similar, the major difference being that the $d$ bands are located 4 eV below the Fermi level in silver and 2 eV below the Fermi level in copper. Both have two peaks in the $d$-band density of states, a sharp peak near the top of the band and a broader peak deeper in the band, and both $d$ bands are approximately 3.5 eV wide. The $p$- and $s$-like bands above and just below the Fermi level appear to be similar. The symmetry points $L_2'$ and $L_1$ differ in energy by less than 0.2 eV. However, the difference between copper and silver in the density of states at $L_2'$, and the difference in the way in which the effect of the direct transition from $L_2'$ to $L_1$ varies with photon energy (Figs. 11 and 36) in addition to the lack of evidence of a peak in the silver density of states at $X_4'$ indicate that the shape of the bands in the two metals is somewhat different. This difference may be due to the fact that the $d$ bands in silver are located further in energy from the symmetry points $L_1$, $L_2'$, and $X_4'$ than the $d$ bands in copper.

The close agreement of the photoemission measurements with theoretical predictions indicates that electron-electron scattering is the strongest inelastic scattering mechanism in both silver and copper for electrons with energies from 1.5 to 11.5 eV above the Fermi level. There is no evidence of scattering due to plasmon creation. The mean free path for electron-electron scattering for copper is a decreasing function of electron energy. From lifetime broadening considerations a value of approximately 75 Å is found for the mean free path against this scattering for electrons 6 eV above the Fermi surface. The mean free path for silver appears to be a more sharply decreasing function of electron energy, and is slightly shorter than that for copper at energies more than 5 eV above the Fermi level.

Close agreement has been obtained between the calculated imaginary part of the dielectric constant $\epsilon_2$ (based on the experimental observation) and the measured $\epsilon_2$. This indicates that the observations are not peculiar to the photoemission process, but are characteristic of the metals studied.

It was possible to explain the photoemission data from both copper and silver in detail. In particular, it was possible to predict the energy distribution of photoemitted electrons to be expected at any photon energy from 1.5 to 11.5 eV with considerable accuracy. It should be pointed out that total agreement between the predicted and the measured distributions could have been achieved by slight changes in the densities of states and matrix elements involved in the transitions. Such adjustments in the data were not made in order to illustrate the ease and accuracy with which photoemission results can be interpreted and the vast amount of information that can be gained without a more detailed analysis.

## ACKNOWLEDGMENTS

The authors are grateful for stimulating discussions with Frank Herman, Neal Kindig, James C. Phillips, and Carver Mead. We are also indebted to Carver Mead, Henry Ehrenreich, Herbert Philipp, and J. C. Phillips for making reports of their work available prior to publication. In addition, we would like to thank Neal Kindig for help in instrumentation and Phillip McKernan for the fabrication of the experimental tubes.

[35] W. E. Spicer, Phys. Rev. Letters 11, 1 (1963).
[36] H. M. Krutter, Phys. Rev. 48, 664 (1935); E. Rudberg and J. C. Slater, *ibid.* 50, 150 (1936).